

Adaptive Extraction Network for Multivariate Long Sequence Time-Series Forecasting

Dandan Zhang^a, Yun Wang^a

^a*School of Computer Science and Engineering, Southeast University, Nanjing, China*

ARTICLE INFO

Keywords:

Deformable convolution
Multi-resolution convolution
Multivariate time-series forecasting

ABSTRACT

Models employing CNN architecture have made significant progress in multivariate long sequence time-series forecasting (MLSTF), particularly in modeling local time series characteristics. However, during the MLSTF process, extracting the global time series patterns and understanding the correlations among different variables are highly significant. To address this challenge, we introduce multi-resolution convolution and deformable convolution operations. By enlarging the receptive field using convolution kernels with different dilation factors to capture temporal correlation information across different resolutions, and adaptively adjusting the sampling positions through additional offset vectors, we enhance the network's ability to capture correlated features between variables. Building upon this, we propose ATVCNet, an adaptive temporal-variable convolutional network designed to effectively model the local/global temporal dependencies and inter-variable dependencies of multivariate time series. Specifically, extracting and fusing time series features at different resolutions, captures both local contextual information and global patterns in the time series. The designed inter-variable feature adaptive extraction module captures the correlation among different variables in the time series. We evaluated the performance of ATVCNet across eight real-world datasets. The results indicate that ATVCNet achieved a performance improvement of approximately 63.4% over state-of-the-art MLSTF models.


1. Introduction

Multivariate long sequence time-series forecasting (MLSTF) stands as one of the most critical challenges in time series analysis, finding extensive applications in fields such as energy [1, 2, 3], data center infrastructure [4], traffic flow [5, 6], finance [7], and more. Its core objective lies in leveraging past time series data to forecast the changing trends of multiple correlated time series over a future time horizon. In recent years, research focus on forecasting methods for multivariate time series has gradually shifted towards Transformer-based models with multi-encoder-decoder architectures and multi-head self-attention mechanisms. This is because Transformer models exhibit strong capabilities in capturing temporal dependencies among long sequences. Consequently, a series of Transformer-based model-driven approaches have emerged, including PatchTST [7], iTransformer [8], and Crossformer [9]. Although Transformer-based models perform well in MLSTF due to their ability to extract temporal information, DLinear [10] and the experiment in Section 4.6 demonstrate that Transformer-based models are often ineffective in capturing global temporal correlations in time series. Additionally, the utilization of self-attention mechanisms at the bottom levels of Transformer-based models for feature extraction leads to high computational costs.

The latest trend in MLSTF research has begun to challenge the efficiency issues of Transformer-based models in prediction tasks. Models like LightTS [11] and DLinear [10], which employ simple linear structures, have shown superior performance in MLSTF compared to the majority of Transformer-based models. However, these models focus on extracting global correlation information in the horizontal time domain, neglecting the understanding of local contextual information and information between different variables, which is crucial for MLSTF. Although TSMixer [12] addresses the issue of extracting cross-variable information by feature dimension transformation and linear mapping, its utilization of fully connected layers for extracting such information leads to information redundancy.

Recently, prediction models based on convolutional modules have shown outstanding performance in MLSTF [13, 14]. These models typically utilize convolutional layers to extract local features from the time series, which to some extent preserve the structural information of the time series. The commonly used convolutional methods for extracting

*Corresponding author

 ywang_cse@seu.edu.cn (Y. Wang)

ORCID(s):

local features include standard convolution and dilated convolution (Figure 1 a,b). The receptive field of standard convolution usually covers only a fixed-size region within the input sequence, exhibiting regularity and fixedness [15], which leads to relatively low variable dependency between regions formed by other sequences. Dilated convolution [14] extends the standard convolution by introducing dilated factor in the convolution kernel, allowing the kernel to span larger receptive fields to capture features at multiple scales. However, dilated convolutions still possess symmetric receptive fields [16], limiting the ability of convolutional layers to perceive features between asymmetric variables, thus presenting certain limitations in capturing sequence dynamics.

To address the aforementioned challenges, we extract relevant features of the time series from both temporal and variable dimensions. Specifically, for capturing the temporal domain information of the time series, we consider extracting local features and patterns at different resolutions within the time series. To extract features between different variables in the time series, we introduce deformable convolutions [17] (Figure 1 c), commonly used in the field of image processing. However, directly applying deformable convolutions to time series prediction tasks may lead to issues of data mismatch and lack of effective learning of temporal intervals.

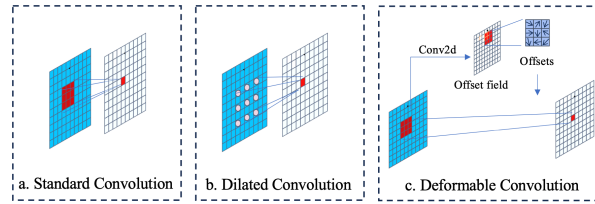


Figure 1: Multiple convolution schemes.

Based on the analysis above, we designed ATVCNet, an adaptive temporal-variable convolutional network, for accurately MLSTF. ATVCNet consists of two key modules: the temporal feature extraction module and the inter-variable feature adaptive extraction module. The temporal feature extraction module extracts local contextual information and patterns at different resolutions by using convolutional kernels with different dilation factors, and ensures the position invariance of the time series through aggregation operations and uses adaptive average pooling layers to establish global pattern information. The inter-variable feature adaptive extraction module utilizes deformable convolutions to adaptively adjust the shape of the convolutional kernel based on the sequence features, extracting correlations between variables in different feature directions and enhancing the model's perception of cross-variable correlations. The main contributions are as follows:

- We propose ATVCNet, an adaptive temporal-variable convolutional network. Experimental studies on 8 real-world datasets demonstrate that the proposed model outperforms the state-of-the-art (SOTA) ConvTimeNet model by 63.4% in terms of MLSTF.
- To extract temporal patterns from the time series, we use convolutions with different dilation factors to extract local contextual features at different resolutions of the input sequence. By overlaying feature information of different resolutions at the same position, we ensure the positional invariance of the input sequence. By employing adaptive average pooling operations, the model gains the capability to extract global feature information from the time series, aiding in capturing overall patterns and trends within the sequence.
- To capture the dependencies among different dimensions, we introduced an inter-variable feature adaptive extraction module. This module employs deformable convolution, which enhances the sampling positions between variables by introducing additional offsets. This allows the network to adaptively adjust the shape of the convolution kernels based on specific data characteristics, thereby capturing features between multivariate data more accurately and significantly reducing redundant features.

The remaining structure of this paper is as follows: In Section 2, we introduce existing methods for time series forecasting and the application of deformable convolutions. Section 3 provides a detailed description of the ATVCNet architecture. Section 4 presents experimental results validating the effectiveness and efficiency of ATVCNet. Finally, in Section 5, we provide a comprehensive summary of the predictive research on the ATVCNet model.

2. Related work

In this section, we delineate the related work into two distinct modules. Section 2.1 provides an overview of prominent contributions within the field of time series forecasting, while Section 2.2 delves into the applications of deformable convolutions in other fields.

2.1. Time modeling in deep time series forecasting

Deep models in time series forecasting can generally be categorized into four paradigms: those based on CNNs, RNNs, Transformers, and MLPs. Models based on CNNs use convolutional kernels along the time dimension to capture local temporal patterns, such as ConvTimeNet [13], MICN [14], SCINet [18], and TCN [19]. On the other hand, models based on RNNs utilize recurrent structures to maintain state propagation, as seen in LSSL [20], LSTNet [21], LSTM [22], etc. However, both of these paradigms suffer from the problem of limited receptive fields, which hampers their ability for long-term forecasting. Recently, Transformer-based models have garnered widespread attention due to their capability in capturing long-range dependencies through attention mechanisms. For instance, models like Autoformer [23], PatchTST [7], ETSformer [24], FEDformer [25], Pathformer [26], and iTransformer [8] adopt the idea of time series decomposition, breaking down time series data into simpler sequential data to handle complex time patterns. SMARTformer [27], Pyraformer [28], and CrossFormer [9] propose new attention mechanisms to enhance prediction accuracy. However, as the forecasting horizon increases, the attention mechanism's extraction capability may diminish. Models based on MLPs utilize simple linear models to extract abstract representations of time series, such as LightTS [11], DLinear [10], TSMixer [12], MLP4Rec [29], FreTS [30] and TimeMixer [31]. However, when dealing with high-dimensional data, the expressive power of linear networks is limited, making them unsuitable for the prediction of multivariate data.

In response to the aforementioned challenge, we developed an efficient module for extracting temporal correlations, which models both global and local aspects.

2.2. Application of deformable convolutions

Deformable convolutions have found widespread application in the field of image processing. In recent research, there has been a growing trend of combining deformable convolutions with attention mechanisms. For instance, in [32, 33], researchers utilized deformable convolutions to capture more important offset information in specific spatial structures, thus providing more precise recognition capabilities. In [34], due to the presence of complex geometric transformations and feature blurring characteristics in the data, researchers employed A2-DCNet modules to capture remote spatial context information from a global perspective. In [35], researchers demonstrated that attention blocks guided by deformable convolutions could acquire semantic information about spatial positions. Additionally, research utilizing deformable convolutions in visual tasks has yielded promising results [36].

These research findings inspire our exploration of deformable convolution patterns in MLSTF. By introducing deformable convolutions into the MLSTF field, we aim to more effectively capture the correlation information among different variables in time series data, thereby enhancing prediction accuracy and performance.

3. Methodology

In this section, we will provide a detailed overview of the ATVCNet architecture. As depicted in Figure 2, the ATVCNet model is designed to effectively extract the time-domain pattern characteristics of time series and complex correlation information between different dimensions from multi-dimensional historical data to achieve accurate long-term prediction of time series. The prediction process of the ATVCNet model mainly consists of the following three stages:

(1) Data processing: For a given multidimensional input dataset, first, standard normalization is applied to eliminate the influence of different resolutions, enhancing the robustness of the model. Subsequently, wavelet denoising is performed on the data to alleviate the interference of noise on model predictions.

(2) Correlation acquisition: It is crucial for accurate MLSTF prediction to adequately extract and utilize both the horizontal time-domain correlation information of the time series and the correlation information among different variables. We employ a temporal feature extraction module and an inter-variable feature adaptive extraction module to extract explicitly correlated features hidden in the original samples, which can significantly enhance prediction accuracy.

(3) Dynamic forecasting: As time progresses, the distribution of time series data in real-world scenarios is likely to change, which may lead to decreased predictive accuracy of the model. Therefore, to maintain the model's performance, it is necessary to recalibrate the model parameters when there is a decline in predictive accuracy. This adjustment helps adapt to the features of new samples, ensuring the model's effectiveness in dynamic forecasting tasks.

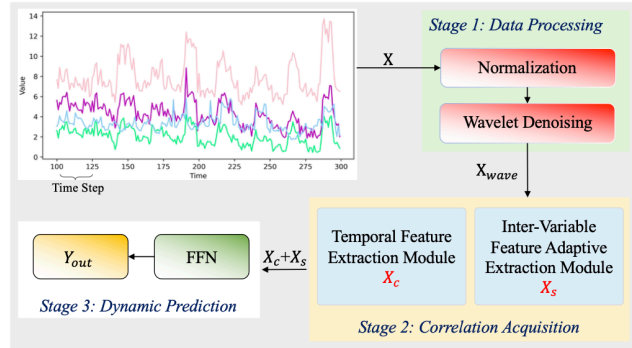


Figure 2: Framework of the ATVCNet.

3.1. Problem statement

In a rolling prediction setup with a fixed-size window, we consider an input sequence denoted as $X = \{x_1, \dots, x_i, \dots, x_m\} \in \mathbb{R}^{M \times N}$, where $x_i = \{x_i^1, \dots, x_i^j, \dots, x_i^N\}$, and x_i^j represents the value of variable j at the i^{th} time point. The objective of long-term prediction for multivariate time series is to forecast $x_{m+L_y} = \{x_{m+1}, \dots, x_{m+L_y}\}$, where the output length L_y represents an extended future time period.

3.2. Data processing

To enhance the robustness of the model, we normalize the data and convert it into time series windows for training and testing. We employ a normalization method to adjust the time series data to a unified scale, expressed as

$$F(i) = \frac{x_i - \mu}{\sigma}, \quad (1)$$

where μ and σ are the mode-wise mean and variance vectors in the training time series.

The accuracy of the model is constrained by the quality of the dataset, which directly impacts the model's predictive outcomes. To enhance the data quality of training samples and mitigate the influence of noisy data on model training, we employ a compromise method between soft and hard thresholds [37]. This method involves filtering based on calculating the optimal denoising threshold, aiming to achieve effective noise reduction.

We assume the presence of a set of data affected by Gaussian white noise, which can be expressed using the following formula:

$$f_i = \theta_i + \varepsilon e_i, \quad (2)$$

where i is the i^{th} sample, $i = 1, 2, \dots, m$, e_i is white noise, θ_i is the data after denoising, and ε is the level of noise.

The following is a detailed description of the wavelet transform thresholding denoising process:

First, perform an orthogonal wavelet transform and select X historical data samples as the input for discrete wavelet transformation. Then, decompose the data into wavelet coefficients up to the j^{th} layer. The wavelet decomposition coefficients $O_{j,k}$ for each layer can be calculated using the following formula:

$$O_{j,k} = \langle f, \Psi_{j,k} \rangle = \int_{-\infty}^{+\infty} f(x) \Psi_{j,k}(t) dt, \quad (3)$$

where f represents the input sequence.

Next, the decomposed wavelet coefficients are subjected to thresholding, where each coefficient is compared with a predefined threshold to obtain the estimated wavelet coefficients. The soft-hard threshold compromise denoising method is expressed as

$$\widehat{O}_{j,k} = \begin{cases} \text{sgn}(O_{j,k}) (|O_{j,k}| - a\gamma), & |O_{j,k}| \geq \gamma, \\ 0, & |O_{j,k}| < \gamma, \end{cases} \quad (4)$$

where $O_{j,k}$ represents the wavelet coefficients obtained from signal decomposition, $\widehat{O}_{j,k}$ represents the wavelet coefficients obtained using the compromise threshold method, γ represents the threshold value of wavelet denoising, $0 \leq a \leq 1$ can obtain a better denoising effect.

Finally, wavelet reconstruction is performed on the estimated wavelet coefficients by using inverse wavelet transform to obtain denoised samples.

$$\widetilde{X}(t) = \sum_{j=-\infty}^{+\infty} \sum_{k=-\infty}^{+\infty} \widehat{O}_{j,k} \Psi_{j,k}. \quad (5)$$

3.3. Temporal-Variable feature extraction

To comprehensively and effectively extract features from time series, we designed the temporal-variable feature extraction module, which consists of two components: the temporal feature extraction module and the inter-variable feature adaptive extraction module, as shown in Figure 3 (a). The former is utilized to capture temporal dependency information of local and global patterns within the time series (as shown in the *Temporal Feature Extraction Module* in Figure 3 (a)), while the latter is employed for effectively extracting correlation information between different variables at various resolutions in the time series (as shown in the *Inter-Variable Feature Adaptive Extraction Module* in Figure 3 (a)).

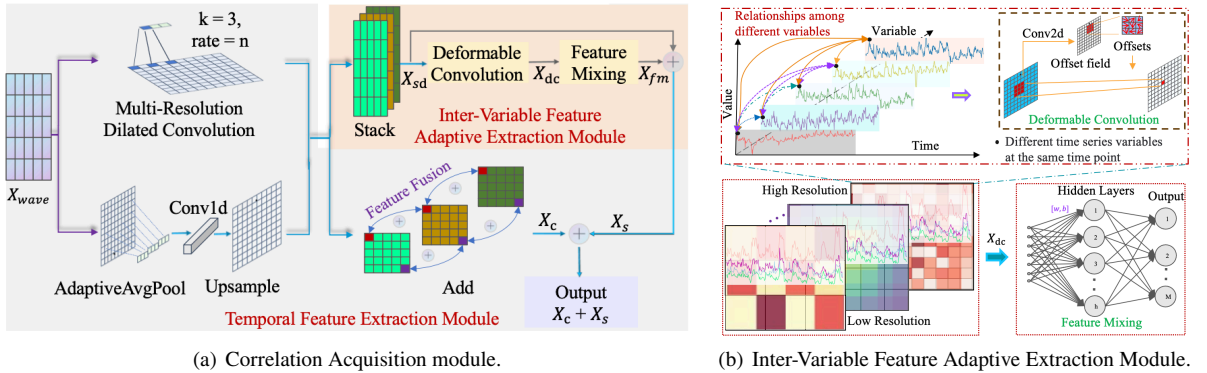


Figure 3: Temporal-Variable feature extraction module.

Temporal Feature Extraction Module Inspired by the concept of SPP [38], the temporal feature extraction module employs one-dimensional (1D) convolutions with varying dilation factors to capture features and patterns at different resolutions within the input multivariate time series data. This approach equips the model with the capability to discern local feature variations: with small dilation factors, the model convolves within a small receptive field, facilitating more precise identification of local patterns and structures, thus aiding in enhancing the network's comprehension of complex patterns. Conversely, with large dilation factors, the model employs larger convolutional kernels to capture features within a broader receptive field, thereby facilitating the identification of local contextual relationships within the input sequence. Additionally, by aggregating feature and pattern information extracted at different resolutions at the same location, it ensures positional invariance of the data during the processing. To encapsulate global trends and patterns, our model incorporates adaptive average pooling operations. This technique is instrumental in distilling the overarching trends and patterns from the time series data, thus enriching the model's comprehensive grasp of the temporal dynamics presented.

When data flows through this module, it is mapped into two tasks: (1) Local feature extraction. By selecting different dilation factors for multi-resolution dilated convolution, the receptive field of the convolutional kernel can be expanded without losing resolution. This module utilizes convolutions of different sizes to learn patterns and local contextual information at different resolutions. (2) Global feature extraction. Introducing global adaptive average pooling effectively captures global information from the entire feature map, aiding the model in better understanding the global patterns and structural information of the entire input sequence. In summary, by overlaying features of different resolutions at the same location, this not only enhances the model's translational invariance but also improves the model's generalization capability through the integration of complementary information. Furthermore, through the designed weight sharing mechanism, the same set of weights is reused across inputs of different resolutions. This not only reduces the number of parameters in the model but also helps to enhance the model's efficiency.

The calculation formula for specific operational steps is as follows:

(1) Given a time series X_{wave} with a length of L , a convolution kernel w with a length of k , and a dilation factor d (by default, $d = 1$), the formula for calculating the 1D dilated convolution is as follows:

$$Conv1d = \sum_{i=1}^k w_i x(t + d \times i), \quad (6)$$

where $Conv1d$ represents the output value at time t , $x(t)$ represents the t -th element in the input sequence, w_i represents the i th element of the convolution kernel w . The calculation formula indicates that at each time t , the output value $Conv1d$ is obtained by weighting and summing the local area of x .

(2) Temporal feature extraction.

$$\begin{aligned} \chi_{dilated} &= Relu(LN(Conv1d(\chi_i^l, d = n))), n \in R, \\ \chi_{avg_pool} &= Upsample(Conv1d(AvgPool(\chi_i^l))). \end{aligned} \quad (7)$$

In the equations, $\chi_{dilated}$ is the result of processing the original data χ_i^l through convolution, linear normalization (LN) and ReLU activation function processing. To balance performance and efficiency, we set the dilated rate $n = \{1, 2, 5\}$ as suggested in [39]. χ_{avg_pool} is the result of adaptive average pooling after up sampling.

Through the aforementioned operations, we capture the local features and pattern information of the time series at different resolutions in $\chi_{dilated}$ and the global information of the time series in χ_{avg_pool} . Then, at the corresponding positions, features from different resolutions at the same time point are fused to obtain the final representation X_c of cross-scale temporal feature information. This design allows the model to obtain contextual information from different temporal scales, providing more perspectives for inference and prediction while ensuring robustness and generalization.

$$X_c = Add(\chi_{dilated}, \chi_{avg_pool}). \quad (8)$$

Inter-Variable Feature Adaptive Extraction Module To effectively extract the correlation and dynamic relationships between different variables under different resolution features of time series, we introduce deformable convolution. By adding additional learnable offsets to standard convolution, it enables the convolutional kernel to adapt to irregular variations in input features, making it particularly suitable for handling complex dynamic relationships between different variables, as illustrated in Figure 3 (b).

Specifically, we stack the extracted multi-resolution feature maps and the output maps from adaptive average pooling into a tensor X_{sd} , which serves as the input to the inter-variable feature adaptive extraction module. We employ deformable convolutions to learn the information between different variables and position offset information in feature graphs with different resolutions, focusing attention on regions with richer information through twist sampling networks. This operation enables the model to more accurately capture and understand dependencies between different dimensions while removing redundant feature information. The mathematical expression of the inter-variable feature adaptive extraction module is as follows:

$$DefConv(p_0) = \sum_{p_n \in R} \mathcal{W}(p_n) \cdot x(p_0 + p_n + \Delta p_n), \quad (9)$$

where $DefConv(p_0)$ is the value of the output feature map at location p_0 . $x(\cdot)$ represents the input feature map. $\mathcal{W}(p_n)$ denotes the weights of the convolutional kernel. Δp_n is the learned offset for each p_n , differing for each point, allowing the convolutional kernel to adaptively adjust its sampling positions on the input feature map. For more detailed

theoretical explanations regarding deformable convolutions, please refer to reference [17]. The inter-variable feature adaptive extraction is described by the following equations:

$$\begin{aligned} X_{sd} &= \text{Stack}(\chi_{dilated}, \chi_{avg_pool}), \\ X_{dc} &= \text{DefConv}(X_{sd}). \end{aligned} \quad (10)$$

Additionally, we implemented a feature mixing layer to integrate the lower-level fine-grained time series information with the higher-level coarse-grained time series information, aiming to merge the correlation information between features at different resolutions. Finally, the use of residual connections allows important feature information to propagate between network layers, preventing information loss. The process is described as follows:

$$\begin{aligned} X_{fm} &= \text{Linear}(X_{dc}), \\ X_s &= X_{sd} + X_{fm}. \end{aligned} \quad (11)$$

In the end, the correlations between different dimensions in the time series are captured in X_s .

3.4. Dynamic prediction

Model forecasting. In the downstream prediction tasks of ATVCNet, we employ a simple feedforward neural network (FFN) architecture. To address potential underfitting issues in regression tasks and improve the computational efficiency of the model, we utilize the Moore-Penrose pseudo-inverse matrix [40] to compute the parameters of the model network quickly. The mathematical expression for the model prediction task is as follows:

$$H(G) = [h_1(x_1), h_2(x_2), \dots, h_L(x_L)], \quad (12)$$

where $G = X_c + X_s$, L is the number of hidden layer nodes, $h_i(x_i) = \text{sigmoid}(w_i x_i + b_i)$ represents the output of the i -th hidden layer node, and $H(G)$ is the output matrix of the hidden layer. The weight matrix β of the output layer is calculated by the least squares method:

$$\beta = (H(G)^T H(G))^{-1} H(G)^T Y, \quad (13)$$

where Y is the target matrix. Ultimately, the output y_i predicted by the model is

$$y_i = \sum_{j=1}^L \beta_j h_j(x_i) = H(G) \beta. \quad (14)$$

Model dynamic updates. As time progresses, the data distribution in real-world applications may change, resulting in a significant deterioration of the model's predictive performance. To address this issue, we extend the model training process to a dynamic update stage. We assume that when the model's predictive performance decreases by 5%, we adopt newly collected samples to retrain the ATVCNet model. It is noteworthy that during this process, we maintain a fixed training set size, which means that when introducing new data, an equal amount of the earliest historical data is removed. This strategy ensures the speed of model training and reduces the required time.

Algorithm 1 outlines the details of the dynamic prediction process.

4. Experiments

In this section, we delve into investigating the effectiveness and efficiency of the ATVCNet network. Through rigorous experimentation across eight authentic datasets, employing fourteen SOTA models, we aim to address the following research inquiries:

- RQ1 (Effectiveness): Can ATVCNet outshine the present SOTA baseline models when applied to real datasets (Sections 4.4 - 4.7)?
- RQ2 (Efficiency): Does ATVCNet exhibit superior performance in terms of resource utilization compared to the current baseline models (Sections 4.8)?

Algorithm 1: Dynamic prediction.**Input:**

- $X = \{x_1, \dots, x_i, \dots, x_m\}$: X denotes the training dataset, where x_i represents the N variable factors at time i .
- 1: **Phase I.** Training the proposed ATVCNet model.
 - 2: **Randomly generated:** The weight ω and the bias vector b between the input layer and the hidden layer in FFN.
 - 3: Data processing X_{wave} is obtained based on formulas (1) to (5).
 - 4: Extract temporal correlation X_c based on formulas (7) to (8)
 - 5: Extract inter-variable correlation X_s based on formulas (10) to (11)
 - 6: Input $X_c + X_s$ into the FFN and calculate β .
 - 7: **Phase II.** Dynamically forecasting the values of a time series.
 - 8: Input the obtained new samples x_j and training data set X into the trained ATVCNet model. If the MSE value exceeds the threshold, update β .

Output: Predicting the trend of changes over a future time period.

Table 1

The key features of the eight time series datasets.

Datasets	Features	Timesteps	Granularity	Information
ETTh1/h2	7	17420	1 hour	Electricity
ETTM1/m2	7	69680	15 min	Electricity
Electricity	321	26304	1 hour	Electricity
Traffic	862	52560	1 hour	Traffic
Exchange	8	7558	1 day	Financial
ILI	7	966	1 week	Medical

- RQ3 (Ablation): To what extent do the distinct components of ATVCNet influence its overall performance in time series forecasting tasks (Sections 4.9)?

4.1. Datasets

We extensively evaluated the proposed ATVCNet model on eight benchmark datasets spanning four real-world fields: energy, finance, medical, and traffic. Table 1 summarizes the key features of these datasets.

- **ETT¹**: The dataset records continuous operation data of power resources over a period of two years, including seven indicators such as oil temperature and load. ETTm1 and ETTm2 denote measurements taken every 15 minutes, while ETTh1 and ETTh2 represent hourly recordings.
- **Electricity²**: The dataset comprises hourly electricity consumption data for 321 customers over two years.
- **Traffic³**: The dataset consists of measurements collected every hour from 862 sensors located on the highways in the San Francisco Bay Area.
- **Exchange⁴**: The dataset records the daily exchange rates of eight different countries over a period of 26 years.
- **ILI⁵**: The dataset collects seven indicators, including the proportion of influenza patients and the total number of patients, from the Centers for Disease Control and Prevention in the United States on a weekly basis.

4.2. Baselines

We selected 14 representative SOTA models that have demonstrated outstanding performance in the field of MLSTF as benchmarks:

¹ETT dataset was acquired at <https://github.com/zhouhaoyi/ETDataset>

²[https://archive.ics.uci.edu/ml/datasets/ElectricityLoadDiagrams 20112014](https://archive.ics.uci.edu/ml/datasets/ElectricityLoadDiagrams+20112014)

³<http://pems.dot.ca.gov>

⁴<https://github.com/laiguo-kun/multivariate-time-series-data>

⁵<https://gis.cdc.gov/grasp/fluview/fluportaldashboard.html>

(1) MLP-based: TimeMixer [31] conducts long-term forecasting by decoupling historical information of complex patterns in multiscale time series. TSMixer [12] combines Patch and MLP, enabling it to extract both temporal correlations and inter-channel correlations. DLinear [10] decomposes time series and utilizes linear network layers for modeling to achieve prediction.

(2) Transformer-based architectures: iTransforemr [8] effectively captures multivariate correlations by independently embedding each variable in the time series as variable sub-tokens. PatchTST [7] employs a channel independence strategy, specifically designed to extract correlations of each channel in multivariate data. Crossformer [9] captures temporal and cross-dimensional dependencies in multivariate time series data by first transforming it into a 2D array and then employing two-stage attention layers. ETSformer [24] and FEDformer [25] both decompose time series data to extract complex patterns. Non-Stationary [41] incorporating sequence stabilization and de-stabilization attention mechanisms to handle non-stationary information.

(3) CNN-based model: ConvTimeNet [13] adaptively segments time series into patches and integrates deepwise convolution and pointwise convolution operations to capture global sequence dependencies and cross-variable interactions. MICN [14] utilizes multi-scale convolution to extract both global and local contextual relationships.

(4) 2D-variation-based: TimesNet [42] converts the 1D temporal dimension into 2D to extract both intra-segment dependencies and dependencies between adjacent segments in time.

(5) Semantic-based model: TS2Vec [43] employs hierarchical contrastive methods on both instance and time dimensions to capture multiscale contextual relationships.

(6) RNN-based model: LSSL [20] simulates basic state space models, utilizing novel parameterization methods to model structured state space sequences, in order to extract longer dependencies.

4.3. Implementation details

Our approach is trained with an initial learning rate of 1×10^{-3} , the convolution dilated rate d for multi-resolution dilated convolution was set to $\{1, 2, 5\}$. The input sequence length for the ILI dataset is $L = 36$, with prediction sequence lengths of $\{24, 36, 48, 60\}$. For other datasets, the input sequence length is $L = 96$, with prediction sequence lengths of $\{96, 192, 336, 720\}$. To verify the robustness of our results, we trained the ATVCNet model with three different random seeds and calculated the mean squared error (MSE) and mean absolute error (MAE) scores using each selected seed. The average results are recorded as shown in Table 2. Additionally, the efficiency of the model is assessed based on floating point operations (FLOPs), Parameters, training time, and Inference time. Experiments are implemented using PyTorch on a single NVIDIA GeForce RTX 3090 24GB GPU, Intel(R) Core(TM) i7-10700k CPU and 32GB RAM.

4.4. Multivariate results and analysis

In the field of multivariate prediction, the ATVCNet framework demonstrates excellent performance on almost all datasets. Through analysis of the result data in Table 2, the following conclusions can be drawn:

- The ATVCNet model significantly improves inference performance on nearly all datasets. As the forecasting horizon increases, the prediction error of ATVCNet shows a gradually stable upward trend, indicating its ability to maintain high long-term robustness in practical applications.
- Compared to the current SOTA forecasting model ConvTimeNet, ATVCNet exhibits notable improvements across various datasets. Specifically, ATVCNet gives 47.9% ($0.319 \rightarrow 0.166$) MSE reduction in ETTm1, 36.9% ($0.211 \rightarrow 0.133$) in ETTm2, 42% ($0.395 \rightarrow 0.229$) in ETTh1, 58% ($0.436 \rightarrow 0.183$) in ETTh2, 32.1% ($0.202 \rightarrow 0.137$) in Electricity, 39.8% ($0.402 \rightarrow 0.242$) in Traffic, 65.7% ($0.347 \rightarrow 0.119$) in exchange and 82.9% ($1.866 \rightarrow 0.319$) in ILI. Overall, ATVCNet yields a 63.4% averaged MSE reduction among above settings. Notably, our model achieved great success on the electricity dataset (321 variables) and the traffic dataset (862 variables), indicating that, compared to the ConvTimeNet model which uses depthwise separable convolutions to extract correlations between different variables, the inter-variable dependency extraction at different resolution scales by ATVCNet is more beneficial for MLSTF.
- ATVCNet outperforms both the iTransformer and TSMixer models significantly. Compared to iTransformer, ATVCNet reduces the MSE across all datasets by 66.8% ($0.576 \rightarrow 0.191$). Similarly, compared to TSMixer, ATVCNet reduces the MSE across all datasets by 49.6% ($0.379 \rightarrow 0.191$). iTransformer and TSMixer both emphasize feature extraction between different variables in time series. While they perform better than models

Table 2

Multivariate results with different prediction lengths. The best results in bold numbers. Avg represents the average value across the four prediction lengths.

Models	ATVCNet (Ours)		ConvTimeNet (2024)		TimeMixer (2024)		iTransformer (2024)		TSMixer (2023)		PatchTST (2023)		MICN (2023)		TimeNet (2023)		Crossformer (2023)		DLinear (2023)		ETSformer (2022)		FEDformer (2022)		Non-Sta (2022)		TS2Vec (2022)		LSSL (2022)		
	MSE	MAE	MSE	MAE	MSE	MAE	MSE	MAE	MSE	MAE	MSE	MAE	MSE	MAE	MSE	MAE	MSE	MAE	MSE	MAE	MSE	MAE	MSE	MAE	MSE	MAE	MSE	MAE	MSE	MAE	
ETTh1	96	0.142	0.263	0.254	0.330	0.320	0.357	0.334	0.368	0.319	0.358	0.324	0.361	0.316	0.362	0.338	0.375	0.428	0.444	0.345	0.372	0.375	0.398	0.379	0.419	0.386	0.398	0.806	0.657	0.450	0.477
	192	0.162	0.282	0.316	0.368	0.361	0.381	0.377	0.391	0.369	0.384	0.362	0.383	0.363	0.390	0.374	0.387	0.445	0.468	0.380	0.389	0.408	0.410	0.426	0.441	0.459	0.444	0.923	0.711	0.469	0.481
	336	0.174	0.295	0.315	0.378	0.390	0.404	0.426	0.420	0.402	0.406	0.390	0.402	0.408	0.426	0.410	0.411	0.533	0.519	0.413	0.413	0.435	0.428	0.445	0.459	0.495	0.464	1.062	0.778	0.586	0.574
	720	0.184	0.304	0.382	0.425	0.454	0.441	0.491	0.459	0.464	0.442	0.461	0.438	0.481	0.476	0.478	0.450	0.728	0.655	0.474	0.453	0.499	0.462	0.543	0.490	0.585	0.516	1.208	0.853	0.635	0.597
	Avg	0.166	0.286	0.319	0.375	0.381	0.395	0.407	0.410	0.389	0.398	0.384	0.396	0.392	0.414	0.400	0.406	0.534	0.522	0.403	0.407	0.429	0.425	0.448	0.452	0.481	0.456	1.000	0.750	0.535	0.532
ETTh2	96	0.111	0.219	0.183	0.265	0.175	0.258	0.180	0.264	0.175	0.256	0.177	0.260	0.179	0.275	0.187	0.267	0.197	0.321	0.193	0.292	0.189	0.280	0.203	0.287	0.192	0.274	1.046	0.810	0.243	0.342
	192	0.129	0.236	0.248	0.305	0.237	0.299	0.250	0.309	0.240	0.230	0.248	0.306	0.307	0.376	0.249	0.309	0.326	0.375	0.284	0.362	0.253	0.319	0.269	0.329	0.280	0.339	2.049	1.108	0.362	0.448
	336	0.140	0.247	0.311	0.345	0.298	0.340	0.311	0.348	0.304	0.338	0.304	0.332	0.325	0.388	0.321	0.351	0.372	0.421	0.369	0.427	0.314	0.357	0.325	0.366	0.334	0.361	2.298	1.199	0.932	0.724
	720	0.152	0.255	0.101	0.396	0.391	0.396	0.412	0.407	0.404	0.398	0.403	0.397	0.502	0.490	0.408	0.403	0.410	0.448	0.554	0.522	0.414	0.413	0.421	0.415	0.417	0.413	2.556	1.317	1.372	0.879
	Avg	0.133	0.239	0.211	0.328	0.275	0.323	0.286	0.332	0.280	0.306	0.283	0.306	0.323	0.382	0.291	0.333	0.326	0.391	0.350	0.401	0.293	0.342	0.305	0.349	0.306	0.347	1.907	1.109	0.735	0.596
ETTh1	96	0.203	0.326	0.338	0.368	0.375	0.400	0.386	0.405	0.381	0.391	0.394	0.408	0.398	0.427	0.384	0.402	0.429	0.440	0.386	0.400	0.494	0.479	0.376	0.419	0.513	0.491	0.602	0.546	0.548	0.528
	192	0.228	0.347	0.377	0.385	0.429	0.421	0.441	0.436	0.433	0.420	0.446	0.438	0.430	0.453	0.436	0.429	0.494	0.482	0.437	0.432	0.538	0.504	0.420	0.448	0.534	0.504	0.663	0.584	0.542	0.526
	336	0.238	0.355	0.400	0.404	0.484	0.458	0.487	0.452	0.472	0.441	0.485	0.455	0.460	0.460	0.491	0.469	0.706	0.625	0.481	0.459	0.574	0.521	0.459	0.465	0.588	0.535	0.729	0.622	1.298	0.942
	720	0.245	0.363	0.465	0.439	0.498	0.482	0.503	0.491	0.485	0.471	0.495	0.474	0.491	0.509	0.521	0.500	0.750	0.689	0.519	0.516	0.562	0.535	0.506	0.507	0.643	0.616	0.846	0.685	0.721	0.659
	Avg	0.229	0.348	0.395	0.399	0.447	0.440	0.454	0.448	0.443	0.431	0.455	0.444	0.445	0.462	0.458	0.450	0.595	0.559	0.456	0.452	0.542	0.510	0.440	0.460	0.570	0.537	0.710	0.609	0.777	0.664
ETTh2	96	0.147	0.259	0.385	0.396	0.289	0.341	0.297	0.349	0.289	0.338	0.302	0.348	0.332	0.377	0.340	0.374	0.632	0.547	0.333	0.387	0.340	0.391	0.358	0.397	0.476	0.458	0.380	0.460	1.616	1.036
	192	0.168	0.279	0.438	0.425	0.372	0.392	0.380	0.400	0.375	0.391	0.388	0.400	0.422	0.441	0.402	0.414	0.676	0.663	0.477	0.476	0.430	0.439	0.429	0.439	0.512	0.493	0.574	0.561	2.083	1.197
	336	0.192	0.295	0.451	0.437	0.396	0.414	0.408	0.432	0.425	0.435	0.426	0.433	0.447	0.474	0.452	0.452	0.924	0.702	0.594	0.541	0.465	0.479	0.496	0.487	0.552	0.551	0.973	0.932	2.970	1.439
	720	0.223	0.310	0.470	0.461	0.412	0.434	0.427	0.445	0.435	0.449	0.431	0.446	0.442	0.467	0.462	0.468	1.390	0.863	0.831	0.657	0.500	0.497	0.463	0.474	0.562	0.560	2.661	1.257	2.576	1.363
	Avg	0.183	0.286	0.436	0.430	0.364	0.395	0.383	0.407	0.381	0.403	0.387	0.407	0.411	0.440	0.414	0.427	0.956	0.694	0.559	0.515	0.439	0.452	0.437	0.449	0.526	0.516	1.147	0.803	2.311	1.259
Electricity	96	0.131	0.233	0.179	0.263	0.153	0.247	0.148	0.240	0.146	0.244	0.195	0.285	0.164	0.289	0.168	0.272	0.254	0.347	0.197	0.282	0.187	0.304	0.193	0.308	0.169	0.273	0.312	0.956	0.300	0.392
	192	0.135	0.239	0.185	0.269	0.166	0.256	0.162	0.253	0.163	0.259	0.199	0.289	0.177	0.285	0.184	0.269	0.261	0.353	0.196	0.285	0.199	0.315	0.201	0.315	0.182	0.286	0.347	0.425	0.297	0.390
	336	0.138	0.245	0.201	0.285	0.185	0.277	0.178	0.269	0.180	0.279	0.215	0.305	0.193	0.304	0.198	0.300	0.273	0.364	0.209	0.301	0.212	0.329	0.214	0.329	0.200	0.304	0.351	0.439	0.317	0.403
	720	0.142	0.250	0.242	0.318	0.225	0.310	0.225	0.317	0.216	0.307	0.256	0.337	0.212	0.321	0.220	0.320	0.303	0.388	0.245	0.333	0.233	0.345	0.246	0.355	0.222	0.321	0.382	0.448	0.338	0.417
	Avg	0.137	0.242	0.202	0.284	0.182	0.272	0.178	0.270	0.176	0.272	0.215	0.304	0.187	0.295	0.193	0.295	0.273	0.385	0.212	0.300	0.206	0.323	0.214	0.327	0.193	0.296	0.348	0.437	0.313	0.401
Traffic	96	0.228	0.286	0.376	0.265	0.462	0.285	0.395	0.268	0.483	0.321	0.544	0.359	0.519	0.309	0.593	0.321	0.558	0.320	0.650	0.396	0.607	0.392	0.587	0.366	0.612	0.338	0.999	0.596	0.798	0.436
	192	0.239	0.292	0.392	0.271	0.473	0.296	0.417	0.276	0.490	0.321	0.540	0.354	0.537	0.315	0.617	0.336	0.572	0.331	0.598	0.370	0.621	0.399	0.604	0.373	0.613	0.340	1.008	0.597	0.849	0.481
	336	0.243	0.300	0.405	0.277	0.498	0.296	0.433	0.283	0.506	0.330	0.551	0.358	0.534	0.313	0.629	0.336	0.587	0.342	0.605	0.373	0.622	0.396	0.621	0.383	0.618	0.328	1.034	0.602	0.828	0.476
	720	0.256	0.307	0.436	0.294	0.506	0.313	0.467	0.302	0.538	0.341	0.586	0.375	0.577	0.325	0.640	0.350	0.652	0.359	0.645	0.394	0.632	0.396	0.626	0.382	0.653	0.355	1.311	0.654	0.854	0.489
	Avg	0.242	0.296	0.402	0.277	0.484	0.297	0.428	0.287	0.504	0.328	0.555	0.362	0.542	0.316	0.620	0.336	0.592	0.338	0.625	0.383	0.621	0.396	0.610	0.376	0.610	0.340	1.034	0.598	0.832	0.471
Exchange	96	0.097	0.083	0.083	0.196	0.100	0.222	0.086	0.206	0.082	0.199	0.082	0.201	0.102	0.235	0.107	0.234	0.329	0.440	0.088	0.218	0.085	0.204	0.148	0.237	0.111	0.237	0.516	0.529	0.395	0.474
	192	0.103	0.177	0.170	0.291	0.129	0.326	0.177	0.299	0.176	0.297	0.187	0.307	0.172	0.316	0.226	0.344	0.544	0.551	0.137	0.316	0.132	0.302	0.271	0.335	0.197	0.317	0.917	0.701	0.776	0.698
	336	0.117	0.316	0.316	0.404	0.379	0.442	0.331	0.417	0.337	0.418	0.345	0.427	0.272	0.407	0.367	0.448	1.017	0.786	0.313	0.427	0.348	0.428	0.460	0.476	0.421	0.476	1.766	1.039	1.029	0.797
	720	0.158	0.817	0.817	0.679	0.904	0.715	0.847	0.691	0.909	0.725	0.887	0.708	0.714	0.658	0.964	0.746	1.239	0.912	0.839	0.695	1.025	0.774	1.195	0.769	1.092	0.769	1.818	0.172	2.283	1.222
	Avg	0.119	0.347	0.347	0.393	0.399	0.426	0.360	0.403	0.376	0.410	0.375	0.411	0.315	0.404	0.416	0.443	0.782	0.681	0.354	0.414	0.410	0.427	0.519	0.454		0.461	0.544	1.268	0.851	1.121
Count	24	0.290	0.311	1.701	0.823	1.212	0.874	2.014	0.899	0.452	0.487	1.724	0.843	2.684	1.112	2.317	0.934	3.041	1.186	2.398	1.040	2.527	1.020	3.278	0.945	2.294	0.				

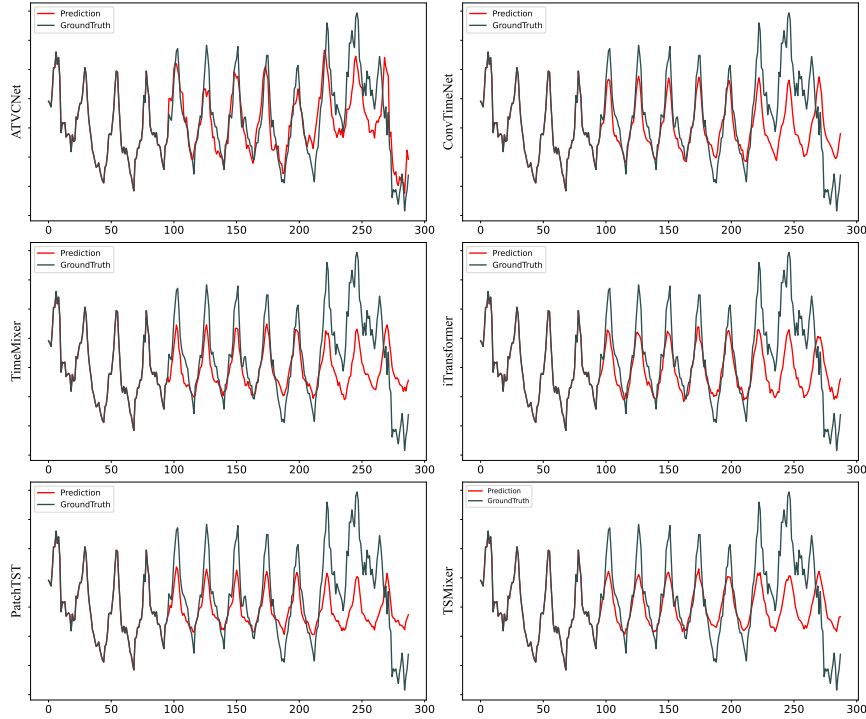


Figure 4: Visualize the ETTh1 dataset, where the first 96 data points represent the input length.

4.6. Long-term information utilization

To validate ATVCNet’s ability to capture long-term correlations, we compared the performance of different models on the ETTh1 and ETTm1 datasets, with output lengths set to {96, 720} and input sequence windows set to {24, 48, 96, 192, 336}. In theory, using longer input sequence windows can increase the receptive field and potentially improve prediction performance. However, as evidenced by the experimental results in Figure 5, the performance of Transformer-based models, TimeMixer, and MICN models does not continuously improve with increasing model input length, indicating that these models do not benefit from longer input sequence windows, i.e., they lack in capturing long-term correlations. In contrast, ATVCNet, ConvTimeNet, and TSMixer show continuous improvement in model performance (decreasing MSE values) with increasing input sequence length, demonstrating that these models can exploit more features from longer input sequence windows and effectively capture the long-term correlations in the input sequence.

4.7. T-tests

To further validate the effectiveness of the ATVCNet model compared to other baseline models, we conducted T-tests to assess the significant differences between the prediction results of ATVCNet and the baseline models. As shown in Figure 6, we can draw the following conclusions: (1) The T-statistic for ATVCNet relative to all baseline models significantly exceeds $T' = 1.782$ (by looking up the critical value in the T-distribution table based on the P-value, we obtain the T-value), indicating that the average MSE of ATVCNet is significantly lower than that of the baseline models. (2) The calculated P-values are all less than the threshold value of $P = 0.05$, indicating statistically significant differences in prediction results among different models. Based on the above analysis, we can conclude that the observed performance differences between ATVCNet and the baseline models are indeed the result of true differences, rather than random factors.

4.8. Efficiency analysis

To evaluate the efficiency of ATVCNet, we selected the ETTh1 dataset and compared it with six SOTA models. We conducted efficiency analysis of the models from four aspects: computational complexity (Flops), model size (Parameters), training time, and inference time. To facilitate a clearer comparison and analysis of model efficiency,

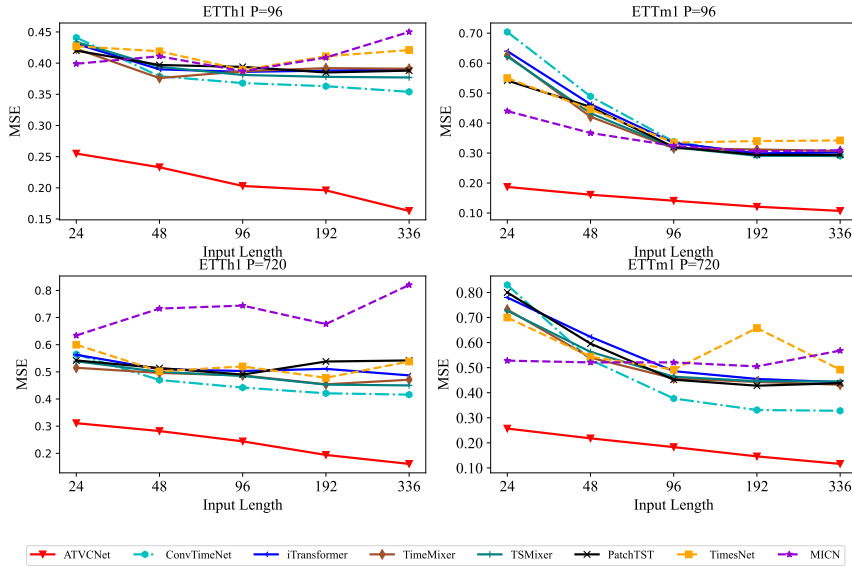


Figure 5: The predictive performance (MSE) of different input sequence windows.

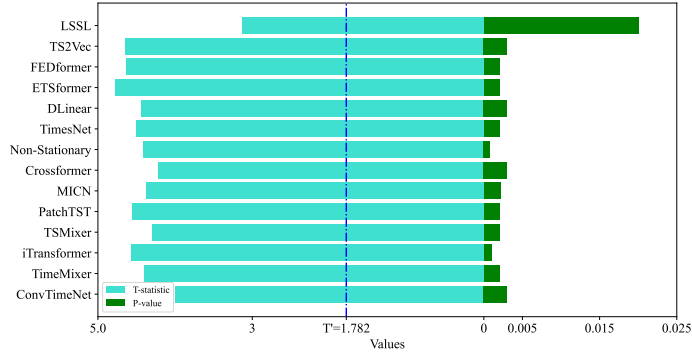


Figure 6: The result of the statistical significance test between ATVCNet and fourteen baseline models.

we integrated these four metrics and computed their average values as the model efficiency scores, as shown in Table 3. Table 3 distinctly demonstrates the efficiency advantages of ATVCNet, which are particularly crucial for practical applications of MLSTF. This advantage mainly stems from the model's parameter sharing mechanism, deformable convolutions, and the ability to rapidly update network weights through pseudo-inverse algorithms. Additionally, we observed a decreasing trend in the training time of iTransformer with increasing input length. This is because iTransformer employs an early termination strategy during training, where training halts when the loss value decreases continuously for a certain number of iterations ($n=3$ in iTransformer). According to our experiments, as the input length increases, the model is more likely to meet this condition during training.

4.9. Ablation study

To assess the effectiveness of each component within ATVCNet, we conducted the following ablations: (1) w/o Variable: removal of modules designed for extracting inter-variable correlation information; (2) w/o Temporal: elimination of modules for extracting temporal correlation information; (3) w/o ALL: complete removal of all feature

Table 3

Results of the efficiency analysis.

Metrics		Flops (G)	Parameters (M)	Training Time (s)	Inference Time (s)	Ranking	
Models						Four Metrics	Avg Ranking
ATVCNet	192	0.064	0.949	20.308	0.091	(1,4,3,1)	2.25
	384	0.128	1.898	35.999	0.124		
	768	0.254	3.700	49.618	0.217		
	1536	0.510	7.589	73.758	0.436		
ConvTimeNet	192	4.745	0.265	14.978	7.977	(4,1,2,7)	3.50
	384	9.491	0.335	24.781	8.975		
	768	18.981	0.476	38.070	10.97		
	1536	37.962	0.757	48.436	13.962		
iTransformer	192	0.305	0.866	1056.093	2.493	(2,2,7,3)	3.50
	384	0.322	0.915	1036.082	2.658		
	768	0.356	1.014	422.610	2.986		
	1536	0.426	1.210	407.591	3.155		
TimeMixer	192	4.329	0.245	14.209	6.979	(6,5,1,6)	4.50
	384	14.895	0.902	17.310	7.978		
	768	54.757	3.464	27.918	8.576		
	1536	209.391	13.571	54.004	9.474		
TSMixer	192	0.027	0.100	38.392	1.723	(3,3,4,2)	3.00
	384	0.087	0.339	41.811	1.931		
	768	0.306	1.239	56.190	1.976		
	1536	1.139	4.727	69.689	2.200		
PatchTST	192	17.253	4.140	51.121	3.649	(5,6,5,4)	5.00
	384	34.505	5.265	80.290	3.936		
	768	69.010	7.515	87.804	4.057		
	1536	138.021	12.015	101.786	3.955		
MICN	192	108.741	27.542	116.441	2.926	(7,7,6,5)	6.25
	384	187.220	36.559	143.929	3.174		
	768	364.311	48.594	174.319	3.823		
	1536	799.024	76.665	273.936	5.757		

extraction modules. We conducted ablation studies on the ETTh2 and Electricity datasets, with input lengths set to 96 and prediction lengths set to {96, 192, 336, 720}.

The results in Table 4 indicate that removing any module from the original model led to a decrease in performance. Specifically: (1) Removing the variable module (w/o Variable) results in the model losing its ability to extract interdependencies among different variables. By solely relying on the the time-domain information extracted by the model, the prediction accuracy of the model is reduced. (2) Removing the temporal domain feature extraction module (w/o Temporal) results in the model's inability to extract long-term trend information and long-term correlations from the time series. Relying solely on the information extracted among different variables by the model also leads to a decline in the model's prediction performance. (3) Completely removing the feature extraction module (w/o ALL) is equivalent to using only the FFN layer for prediction. Experimental results indicate that this approach performs poorly, once again demonstrating that FFN lacks the ability to effectively extract complex features from time series data.

5. Conclusion

This paper introduces ATVCNet, an adaptive temporal-variable convolutional network. From both the temporal and variable dimensions, we utilize convolutional kernels with different dilation factors to capture underlying local patterns and features at different resolutions within complex time series. Additionally, we employ adaptive average pooling to learn global temporal patterns. Leveraging the flexibility of deformable convolutions, the network can effectively capture correlations and dynamics between different variables. Furthermore, considering the inherent variability in the data distribution of time series, the model allows for dynamic updates based on changes in the data.

Table 4

Results of the ablation study.

Models		ATVCNet		w/o Variable		w/o Temporal		w/o All	
Metric		MSE	MAE	MSE	MAE	MSE	MAE	MSE	MAE
ETTh2	96	0.147	0.259	0.156	0.267	0.171	0.276	0.185	0.287
	192	0.168	0.279	0.180	0.287	0.203	0.300	0.226	0.315
	336	0.192	0.295	0.205	0.304	0.236	0.319	0.269	0.337
	720	0.223	0.310	0.237	0.320	0.277	0.340	0.325	0.363
	Avg	0.183	0.286	0.195	0.295	0.222	0.309	0.251	0.326
Electricity	96	0.131	0.233	0.136	0.238	0.141	0.243	0.144	0.246
	192	0.135	0.239	0.144	0.249	0.143	0.247	0.146	0.250
	336	0.138	0.245	0.153	0.255	0.148	0.253	0.151	0.257
	720	0.142	0.250	0.155	0.257	0.150	0.255	0.153	0.258
	Avg	0.137	0.242	0.147	0.250	0.146	0.250	0.149	0.253

Through extensive experimentation on eight benchmark datasets, our findings demonstrate the superior performance of ATVCNet compared to previous SOTA models.

Acknowledgments

This work is partially supported by National Hi-Tech Project, China with grant No. WDZC20215250117.

References

- [1] J. Ye, W. Li, Z. Zhang, T. Zhu, L. Sun, B. Du, Mvts-library: An open library for deep multivariate time series forecasting, *knowl.-Based Syst.* 283 (2024).
- [2] Graphformer: Adaptive graph correlation transformer for multivariate long sequence time series forecasting, *knowl.-Based Syst.* 285 (2024) 111321.
- [3] S. Kim, E. Chung, P. Kang, Feat: A general framework for feature-aware multivariate time-series representation learning, *knowl.-Based Syst.* 277 (2023) 110790.
- [4] F. Shen, J. Wang, Z. Zhang, X. Wang, Y. Li, Z. Geng, B. Pan, Z. Lu, W. Zhao, W. Zhu, Long-term multivariate time series forecasting in data centers based on multi-factor separation evolutionary spatial-temporal graph neural networks, *knowl.-Based Syst.* 280 (2023) 110997.
- [5] A lightweight multi-layer perceptron for efficient multivariate time series forecasting, *knowl.-Based Syst.* 288 (2024) 111463.
- [6] Y. Jin, K. Chen, Q. Yang, Transferable graph structure learning for graph-based traffic forecasting across cities, in: *Proceedings of the 29th ACM SIGKDD Conference on Knowledge Discovery and Data Mining*, 2023, pp. 1032–1043.
- [7] Y. Nie, N. H. Nguyen, P. Sinthong, J. Kalagnanam, A time series is worth 64 words: Long-term forecasting with transformers, in: *The Eleventh International Conference on Learning Representations*, 2023.
- [8] Y. Liu, T. Hu, H. Zhang, H. Wu, S. Wang, L. Ma, M. Long, itransformer: Inverted transformers are effective for time series forecasting, *arXiv preprint arXiv:2310.06625* (2023).
- [9] M. Hassanin, A. Khamiss, M. Bennamoun, F. Boussaid, I. Radwan, Crossformer: Cross spatio-temporal transformer for 3d human pose estimation, *arXiv preprint arXiv:2203.13387* (2022).
- [10] A. Zeng, M. Chen, L. Zhang, Q. Xu, Are transformers effective for time series forecasting?, in: *Proceedings of the AAAI conference on artificial intelligence*, volume 37, 2023, pp. 11121–11128.
- [11] T. Zhang, J. Bian, Y. Zhang, X. Yi, J. Li, W. Cao, S. Zheng, Less is more: Fast multivariate time series forecasting with light sampling-oriented mlp structures, 2022.
- [12] V. Ekambaram, A. Jati, N. Nguyen, P. Sinthong, J. Kalagnanam, Tsmixer: Lightweight mlp-mixer model for multivariate time series forecasting, in: *Proceedings of the 29th ACM SIGKDD Conference on Knowledge Discovery and Data Mining*, KDD '23, 2023, pp. 459–469.
- [13] M. Cheng, J. Yang, T. Pan, Q. Liu, Z. Li, Convtimenet: A deep hierarchical fully convolutional model for multivariate time series analysis, *arXiv preprint arXiv:2403.01493* (2024).
- [14] H. Wang, J. Peng, F. Huang, J. Wang, J. Chen, Y. Xiao, Micn: Multi-scale local and global context modeling for long-term series forecasting, in: *The Eleventh International Conference on Learning Representations*, 2022.
- [15] J. Yang, A. Li, J. Qian, J. Qin, L. Wang, A hyperspectral image classification method based on pyramid feature extraction with deformable-dilated convolution, *IEEE Geosci. and Remote Sens. Lett.* 21 (2024).
- [16] W. Zeng, C. Lin, K. Liu, J. Lin, A. K. H. Tung, Modeling spatial nonstationarity via deformable convolutions for deep traffic flow prediction, *IEEE Trans. on Knowl. and Data Eng.* 35 (2023) 2796–2808.
- [17] J. Dai, H. Qi, Y. Xiong, Y. Li, G. Zhang, H. Hu, Y. Wei, Deformable convolutional networks, in: *2017 IEEE International Conference on Computer Vision (ICCV)*, 2017.

- [18] M. Liu, A. Zeng, M. Chen, Z. Xu, Q. Lai, L. Ma, Q. Xu, Scinet: Time series modeling and forecasting with sample convolution and interaction, volume 35, 2022.
- [19] J.-Y. Franceschi, A. Dieuleveut, M. Jaggi, Unsupervised scalable representation learning for multivariate time series, Le Centre pour la Communication Scientifique Directe - HAL - Diderot (2019).
- [20] A. Gu, K. Goel, C. Ré, Efficiently modeling long sequences with structured state spaces, arXiv preprint arXiv:2111.00396 (2021).
- [21] G. Lai, W.-C. Chang, Y. Yang, H. Liu, Modeling long- and short-term temporal patterns with deep neural networks, in: ACM/SIGIR Proceedings 2018, 2018, pp. 95–104.
- [22] A. Graves, Supervised sequence labelling with recurrent neural networks, 2012.
- [23] H. Wu, J. Xu, J. Wang, M. Long, Autoformer: Decomposition transformers with auto-correlation for long-term series forecasting, volume 27, 2021, pp. 22419–22430.
- [24] G. Woo, C. Liu, D. Sahoo, A. Kumar, S. Hoi, Etsformer: Exponential smoothing transformers for time-series forecasting, arXiv preprint arXiv:2202.01381 (2022).
- [25] T. Zhou, Z. Ma, Q. Wen, X. Wang, L. Sun, R. Jin, Fedformer: Frequency enhanced decomposed transformer for long-term series forecasting, in: International conference on machine learning, 2022, pp. 27268–27286.
- [26] P. Chen, Y. Zhang, Y. Cheng, Y. Shu, Y. Wang, Q. Wen, B. Yang, C. Guo, Pathformer: Multi-scale transformers with adaptive pathways for time series forecasting, 2024.
- [27] Y. Li, S. Qi, Z. Li, Z. Rao, L. Pan, Z. Xu, Smartformer: Semi-autoregressive transformer with efficient integrated window attention for long time series forecasting, in: Proceedings of the Thirty-Second International Joint Conference on Artificial Intelligence, IJCAI-23, 2023, pp. 2169–2177. doi:10.24963/ijcai.2023/241.
- [28] S. Liu, H. Yu, C. Liao, J. Li, W. Lin, A. X. Liu, S. Dustdar, Pyraformer: Low-complexity pyramidal attention for long-range time series modeling and forecasting, 2022.
- [29] M. Li, X. Zhao, C. Lyu, M. Zhao, R. Wu, R. Guo, Mlp4rec: A pure mlp architecture for sequential recommendations (2022).
- [30] K. Yi, Q. Zhang, W. Fan, S. Wang, P. Wang, H. He, D. Lian, N. An, L. Cao, Z. Niu, Frequency-domain mlps are more effective learners in time series forecasting, ArXiv abs/2311.06184 (2023).
- [31] S. Wang, H. Wu, X. Shi, T. Hu, H. Luo, L. Ma, J. Y. Zhang, J. ZHOU, Timemixer: Decomposable multiscale mixing for time series forecasting, in: The Twelfth International Conference on Learning Representations, 2024.
- [32] L. Dai, G. Zhang, R. Zhang, Radanet: Road augmented deformable attention network for road extraction from complex high-resolution remote-sensing images, IEEE Trans. on Geosci. and Remote Sens. 61 (2023).
- [33] S. Zhuo, J. Zhang, Attention-based deformable convolutional network for chinese various dynasties character recognition, Expert Syst. With Appl. 238 (2024).
- [34] J. Du, W. Fan, C. Gong, J. Liu, F. Zhou, Aggregated-attention deformable convolutional network for few-shot sar jamming recognition, Pattern Recognit. 146 (2024).
- [35] J. Luo, P. Huang, P. He, B. Wei, X. Guo, H. Xiao, Y. Sun, S. Tian, M. Zhou, P. Feng, Dca-daffnet: An end-to-end network with deformable fusion attention and deep adaptive feature fusion for laryngeal tumor grading from histopathology images, IEEE Trans. on Instrum. and Meas. 72 (2023).
- [36] C. Ma, L. Zhuo, J. Li, Y. Zhang, J. Zhang, Cascade transformer decoder based occluded pedestrian detection with dynamic deformable convolution and gaussian projection channel attention mechanism, IEEE Trans. on Multimed. 25 (2023) 1529–1537.
- [37] C. Wei, Z. Mu, M. W. Bhatt, Railway foreign body vibration signal detection based on wavelet analysis, J. of Vibroengineering 24 (2022) 1139–1147.
- [38] K. He, X. Zhang, S. Ren, J. Sun, Spatial pyramid pooling in deep convolutional networks for visual recognition, IEEE Trans. on Pattern Anal. & Mach. Intell. 37 (2015) 1904–1916.
- [39] C. Li, Z. Qiu, X. Cao, Z. Chen, H. Gao, Z. Hua, Hybrid dilated convolution with multi-scale residual fusion network for hyperspectral image classification, Micromachines 12 (2021) 545.
- [40] J. A. Vázquez-Coronel, M. Mora, K. Vilches, A review of multilayer extreme learning machine neural networks, Artif. Intell. Rev. 56 (2023) 13691–13742.
- [41] Y. Liu, H. Wu, J. Wang, M. Long, Non-stationary transformers: Exploring the stationarity in time series forecasting, Adv. in Neural Inf. Process. Syst. 35 (2022) 9881–9893.
- [42] H. Wu, T. Hu, Y. Liu, H. Zhou, J. Wang, M. Long, Timesnet: Temporal 2d-variation modeling for general time series analysis, in: The eleventh international conference on learning representations, 2022.
- [43] Z. Yue, Y. Wang, J. Duan, T. Yang, C. Huang, Y. Tong, B. Xu, Ts2vec: Towards universal representation of time series, in: Proceedings of the AAAI Conference on Artificial Intelligence, volume 36, 2022, pp. 8980–8987.